

# Automated Monitoring of Livestock Behavior Using Frequency-Modulated Continuous-Wave Radars

Dominique Henry<sup>1, 2, \*</sup>, Hervé Aubert<sup>1, 2</sup>, Edmond Ricard<sup>3</sup>,  
Dominique Hazard<sup>3</sup>, and Mathieu Lihoreau<sup>4</sup>

**Abstract**—In animal production, behavioral selection is becoming increasingly important to improve the docility of livestock. Several behavioral traits, including motion, are experimentally recorded in order to characterize the reactivity of animals and investigate its genetic determinism. Behavioral analyses are often time consuming because large numbers of animals have to be compared. For this reason, automatization is needed to develop high throughput data recording and efficient phenotyping. Here we introduce a new method to monitor the position and motion of an individual sheep using a 24 GHz frequency-modulated continuous-wave radar in a classical experimental paradigm called the *arena test*. The measurement method is non-invasive, does not require equipping animals with electronic tags, and offers a depth measurement resolution less than 10 cm. Parasitic echoes (or “clutters”) that could alter the sheep backscattered signal are removed by using the singular value decomposition analysis. In order to enhance the clutters mitigation, the direction-of-arrivals of electromagnetic backscattered signals are derived from applying the MUltiple Signals Classification algorithm. We discuss how the proposed automatized monitoring of individual sheep could be applied to a wider range of species and experimental contexts for animal behavior research.

## 1. INTRODUCTION

Over recent years, advances in quantitative methods for the study of animal behavior have allowed the development of high throughput behavioral analyses (sometimes called *ethomics* [1], with applications in neurosciences [2], ethology [3], ecology [4], conservation [5], genetics [6], welfare [7], and farming [8]. In agronomy research, analyses of social behavior in livestock are particularly important in order to improve breeding programs. This includes animal-to-animal interactions (for same or different breeds, gender or age) and animal-to-human interactions. A deep understanding of these interactions can facilitate animals adaptation to farming, improve their robustness, their welfare, and ease the work of farmers [9]. Studies have already shown that the social behavior of a sheep can be genetically selected through generations [10] and could be integrated in the future as new selection criteria for the farming sector. The analysis of social behavior requires recording different parameters, such as the position of the animal, its motion, and the time spent performing different behaviors, in standard experimental conditions [11].

In order to extend genetic selection on commercial farms, the system for behavioral quantification must be low cost, automated, and easy to handle for analyzing a large number of animals (often a thousand or more). A very few solutions exist to perform such analysis in farming conditions. Currently

---

Received 4 April 2018, Accepted 6 June 2018, Scheduled 15 June 2018

\* Corresponding author: Dominique Henry (dhenry@laas.fr).

<sup>1</sup> LAAS-CNRS, MINC, Toulouse 31031, France. <sup>2</sup> University of Toulouse INP, France. <sup>3</sup> GenPhySE UMR1388, INRA, ENVT, Castanet Tolosan, France. <sup>4</sup> Research Center on Animal Cognition, Center for Integrative Biology; CNRS, University Paul Sabatier — Toulouse III, France.

these individual measures are recorded manually by an experimenter, or by video analysis. It is time-consuming and has high risks of subjective interpretations. To our knowledge, no automated systems with required specifications are commercially available. Existing solutions are prototypes embedded on animals, and are composed of multiples sensors, such as accelerometers [12] or GPS (Global Positioning System) navigation devices [13]. Such sensors are invasive, active (i.e., they require their own battery) with a non-negligible cost, and they may alter the animal behavior. Radar systems have been used for tracking small animals, such as low flying insects (honey bees [14], bumblebees [15], hornets [16], butterflies [17]), ground walking invertebrates (beetles and snails [18]) and vertebrates (frogs [19]). So far however, this approach has required the use of harmonic radars, which are expensive, difficult to transport, restrained to tracking one or few individuals simultaneously, and have relatively poor time (3 seconds) and spatial (1 meter) resolution.

In the context of animal selection, sheep behavior is often analyzed using a standard protocol, referred as the *arena test* [20] which consists in quantifying the activity of an animal in an open space. Here we introduce a new solution for the automated monitoring of sheep behavior by means of a 24 GHz FM-CW (Frequency-Modulated Continuous-Wave) radar and validate our approach in the arena test. Microwave FM-CW radars are effective for short-range applications (< 100 meters) with fine spatial resolutions (< 10 centimeters). In contrast to harmonic radars or bioimplantable devices [21], no embedded sensors or tags are needed because the detection is based on the electromagnetic backscattering from the animal. Moreover, the reader system is low-cost (< \$500), portable (dimensions of ten centimeters) and easy to install.

First, we briefly describe the standard arena test protocol and discuss its drawbacks and advantages. Then, we report the radar tracking of a single sheep moving in the arena. We propose an original and efficient step-by-step methodology for removing, or at least significantly reducing, undesirable radar echoes or spots in the radar image. These echoes originate in the electromagnetic backscattering from the stationary arena walls, and their mitigation is performed here from using the Singular Value Decomposition (SVD) technique. We show here that it is possible to partially remove such undesirable clutter by estimating the direction-of-arrivals of electromagnetic signals which are backscattered from the scene. This estimation is based on the MULTiple SIGNALS Classification (MUSIC) algorithm. Next, the remote tracking of two moving animals (a ewe and a lamb) is reported.

## 2. MATERIALS AND METHODS

The experiments described here fully comply with applicable legislation on research involving animal subjects in accordance with the European Union Council directive (2010/63/UE). The investigators carrying out the experiments were certified by the relevant French governmental authority. All experimental procedures were done under guidelines for the care and use of experimental animals established by the French Ministry of Agriculture ethics policy. The experimental animals were reared under usual semi-intensive conditions.

## 3. THE STANDARD ARENA TEST PROTOCOL

The arena test protocol allows analyzing a large panel of animal behaviors, including the animal motion, in a closed area and in different social conditions. Following Ligout et al. [20], the test consists in two social phases named (a) social-attraction and (b) social-isolation, where vocal and locomotor reactivity of the sheep are measured in different conditions (alone, with conspecifics, food, or humans) standing usually at the end of the arena behind a door or a fence.

All measures were conducted in April 2017 at an experimental farm of the Institut National de la Recherche Agronomique (Lanlade, France). We conducted all the experiments on two sheep (*Ovis aries*) of different sizes: a ewe (2 years old, longer than 1 meter) displayed on Figure 1(a) and a lamb (1.5 months old, 50 centimeters long). The radar and its antennas were located in front of the arena test (length = 12 meters, width = 2 meters). For each measure we released the sheep in the arena for 1 minute and recorded the sheep position every 100 ms. A camera (400 × 320 pixels) was placed next to the antennas in order to compare the positions provided by the radar with the observed location of the animal.

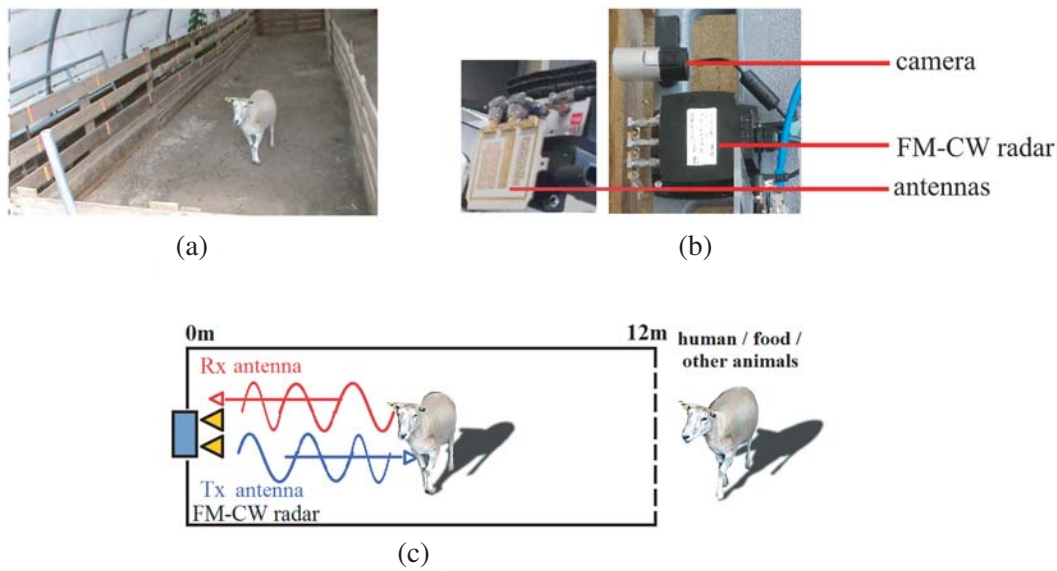


**Figure 1.** (a) Picture of the arena ( $2 \times 12$  meters) with a ewe inside and (b) camera and FM-CW radar system measurement (DK-sR-1030e model from IMST GmbH) located in front of the arena. (c) Arena test configuration including the FM-CW radar system at the front of the arena. Transmitting and receiving radar antennas are denoted respectively by Tx-antenna and Rx-antenna.

#### 4. RADAR TRACKING OF SHEEP

The proposed technique is based on the periodic acquisition of radar images of a moving target (ewe or lamb) in the arena. As panel walls are stationary while the target is animated, the processing of the difference between radar images obtained at consecutive time steps is expected to help discriminating the target echo from the wall clutter. However many undesirable electromagnetic backscatterings from the scene may render this discrimination very challenging. One of the main issues is the strong clutter induced by the panel walls that delimit the arena. If the target is too close to the walls, this clutter obscures the echo of the target. Spurious echoes detection due to multi-path electromagnetic propagation may provide undesirable time-varying spot in the radar image and generate false target detections. The target hides various parts of the wall during the radar tracking and, consequently, the wall clutter may wrongly be viewed as a non-stationary target. Therefore, an effective technique is required to discriminate in the radar image the echo from panel walls and the echo from the moving target.

We propose here a clutter mitigation technique for the radar ranging of non-stationary targets in the arena. This new method allows to reduce significantly the clutter and clearly reveals the variation in time of variable target range. The proposed step-by-step technique first periodically measures the radar signal of the scene. A matrix is then built from the time signal vectors recorded during the entire experiment and the singular values of this matrix are computed. We show that the singular components from a specific index span a multidimensional subspace from which the time-variation of the target range can be accurately estimated. The steps of the proposed methodology are described below.

##### 4.1. Step n<sup>o</sup>1: Building the Signal Matrix from the Periodic Radar Interrogation of the Scene

The microwave radar used here is qualified as a short-range [22] ( $< 100$  meters) Frequency-Modulated Continuous-Wave (FM-CW) radar (DK-sR-1030e model from IMST GmbH). It has two separated channels for transmitting and receiving radar echoes. A  $1 \times 5$  patches array antenna (gain of 11 dBi and beamwidths of  $55^\circ$  in azimuth and  $22^\circ$  in elevation) is used for periodically illuminating the scene

with a FM microwave signal called the “chirp” [23]. The chirp is here characterized by its carrier frequency of 23.8 GHz, the modulation bandwidth  $B$  of 2 GHz, and the up-ramp modulation duration  $T_M$  of 5 milliseconds. The output microwave power at the radar front-end is of 20 dBm (100 milliwatts). At reception, two  $1 \times 5$  patches array antennas (beamwidths of  $60^\circ$  and  $70^\circ$  in azimuth and  $25^\circ$  in elevation) are used. The separation distance between these two antennas is of 6 mm. Pictures of the measurement system and the arena test configuration are displayed on Figures 1(b) and (c). At time  $t_k = k \cdot T$  where  $k = 1, 2, \dots, K$  (in our experiment  $T = 100$  milliseconds and  $K = 100$ ), the  $k$ th measurement is performed as follows: one chirp is transmitted, then it is backscattered by the scene and is finally received by the radar. Next, the received signal is multiplied in time-domain by the transmitted chirp and the resulting signal  $s_k$  is placed in the  $k$ th row of the signal matrix denoted by  $\mathbf{S}$ . After  $K$  consecutive measurements, the dimension of this matrix is of  $K \times N$ , where  $N$  is the number of time samples used for each measurement of signal  $s_k$ .

#### 4.2. Step n°2: Singular Value Decomposition of the Signal Matrix

Following the Singular Value Decomposition (SVD) technique [24], the matrix  $\mathbf{S}$  built at the previous step can be decomposed as  $\mathbf{U}\Sigma\mathbf{V}^H$  where the  $K \times K$  matrix  $\mathbf{U}$  and  $N \times N$  matrix  $\mathbf{V}$  are unitary matrices containing respectively left and right singular vectors and  $\mathbf{V}^H$  is the Hermitian transpose of  $\mathbf{V}$ . The  $K \times N$  matrix  $\Sigma$  contains singular values  $\sigma_n$  for  $n = 1, 2, \dots, N$  in its diagonal ( $\sigma_1 \geq \sigma_2 \geq \dots \geq \sigma_N$ ). Without animal in the arena, the scene is stationary and all measured signals  $s_1, s_2, \dots, s_K$  are theoretically identical. In this specific case, the rank of the signal matrix is equal in theory to one and consequently, there is only one nonzero singular value  $\sigma_1$ . As a consequence, the signal which is backscattered from the scene is expected to span a one-dimensional subspace. When a target (sheep) is in the arena, the signals  $s_1, s_2, \dots, s_K$  are no more identical and consequently, the scene is not characterized by a single singular value, but by a set of values  $\sigma_1, \sigma_2, \dots, \sigma_K$ , as illustrated on Figure 2. This set of non-zero singular components, generated by a moving or static animal, produces a distortion of the wall subspace and spans a multidimensional subspace. The magnitude of this distortion is expected to be related to the range of the target from the radar.

The signal  $s_k$  measured at time  $t_k$  can be expressed as the superposition of the wall and target electromagnetic backscattering. However, if the wall backscattering is significantly higher than the

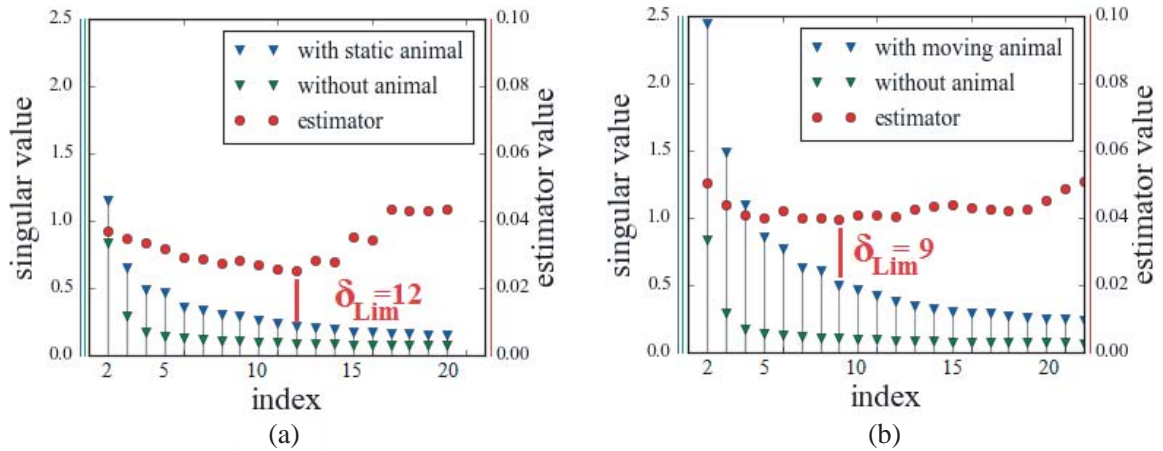


**Figure 2.** Singular values (the first one  $\sigma_1$  is not reported in the figure for clarity purpose) when the animal is present (blue symbols) or absent (green symbols) in the arena. The singular value components span a multi-dimensional subspace which depends on range of the animal from the radar. These components are given for (a) a static animal and (b) a moving animal. As these two spectra significantly differ, singular value components could be at least used for estimating if the animal is moving or not. The values of the statistical estimator defined in the step n°3 (see text) and represented by red circles will be used to determine the singular value limit  $\delta_{Lim}$  and retrieve the animal position.

target backscattering, the wall backscattering can be assumed to lie in a subspace spanned by the first singular components. Therefore, removing such components from the signal matrix may suppress, or significantly reduce, the wall clutter. The number  $\delta$  of first leading singular values to be removed from the signal matrix can be derived from the experimental approach described in the next step.

### 4.3. Step n°3: Experimental Derivation of the Number of Dominant Singular Values to Remove from the Signal Matrix for Reducing the Wall Clutter

Let  $\tilde{s}_k$  be the Fourier transform of the signal  $s_k$  measured at step n°1. The resulting spectrum is called the beat frequency spectrum at time  $t_k$ . If the animal is located at the range  $R$  from the radar, it may generate a peak in this spectrum at the beat frequency  $\frac{2 \cdot B \cdot R}{T_M \cdot c}$ , where  $c$  is the light velocity in vacuum [23]. The consecutive measurements of beat frequency spectra  $\tilde{s}_1, \tilde{s}_2, \dots, \tilde{s}_K$  are respectively placed at the first, second, ...  $k$ th rows of the spectral matrix  $\tilde{\mathbf{S}}$ . Figure 3(a) shows the image of the resulting matrix. Clearly, the wall electromagnetic backscattering dominates the image and obscures the target echo.

Let  $\tilde{\mathbf{S}}_\delta$  be the spectral matrix resulting from removing the first leading singular components  $\sigma_1, \sigma_2, \dots, \sigma_\delta$  to the matrix  $\mathbf{S}$ . Figure 3(b) presents the image of matrix  $\tilde{\mathbf{S}}_{\delta=1}$ . A low-pass filter (Butterworth type) was applied at each range to remove lower spurious echoes (the cut-off range is set to 1.5 meter). Only the first dominant singular value is removed, but it is not sufficient to clearly estimate the animal position. As shown on Figure 3(c), removing the first seventeen dominant singular components  $\sigma_1, \sigma_2, \dots, \sigma_{17}$  eliminates most of the wall reflections and the electromagnetic echo of the sheep is enlightened. Moreover, as shown in Figure 3(d), the clutter mitigation is no more improved when  $\delta$  is higher than 17.

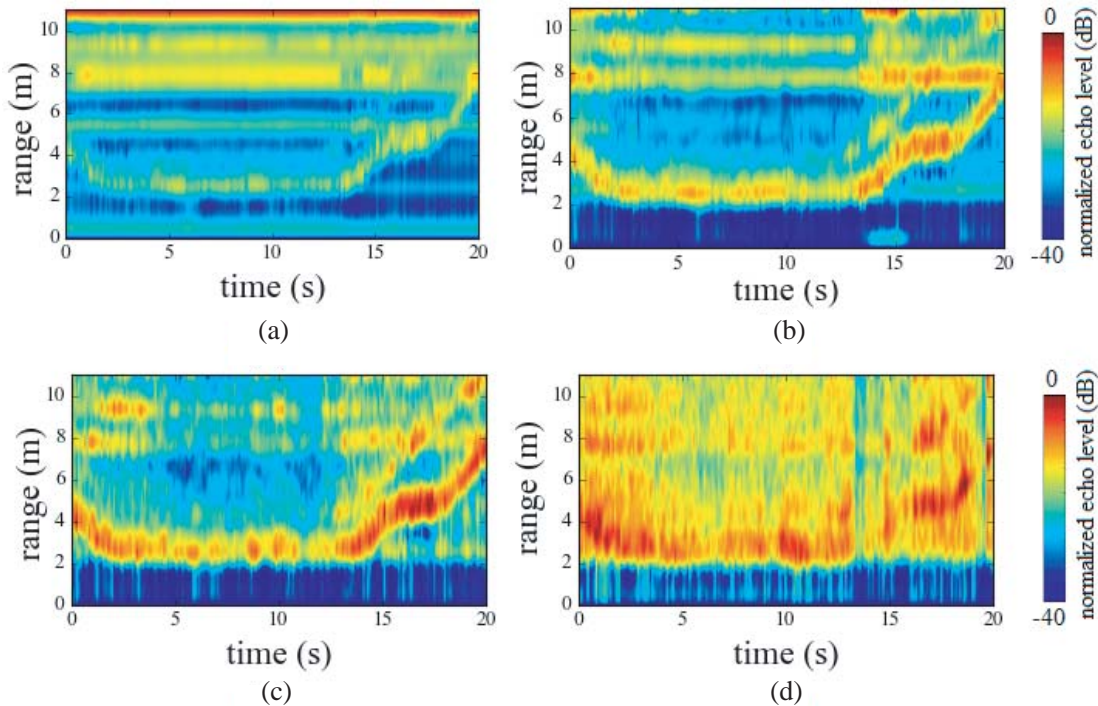


**Figure 3.** (a) Image of the matrix  $\tilde{\mathbf{S}}$ , including all singular values. The wall electromagnetic backscattering is dominant in comparison with the backscattering of the sheep ( $e_N = 9.1 \times 10^{-2}$ ); (b) Image of the matrix  $\tilde{\mathbf{S}}_{\delta=1}$ , i.e., without the first singular value ( $e_N = 4.4 \times 10^{-2}$ ); (c) The first seventeen singular values are removed ( $\delta = 17$ ) and as a result, the echo of the sheep is dominant ( $e_N = 3.3 \times 10^{-2}$ ); (d) As expected, for larger values of  $\delta$  ( $\delta = 90$  in this figure), noise tends to be dominant ( $e_N = 7.8 \times 10^{-2}$ ).

A systematic criterion for predicting the number of singular components to be removed and minimizing the wall clutter would be helpful. For stationary scenes, this optimal number for wall clutter mitigation seems to exist [25]. In the present case, different subspace distortions take place when the animal moves or is static (see step n°2 above). To overcome this problem, the singular values are calculated in a sliding window of 100 signal samples. An estimator  $e_N$  (red circles on Figure 2) is defined as the ratio between the mean echo level of the total scene over the maximal echo level. A low value of  $e_N$  corresponds to a high signal-to-noise ratio. The matrix  $\tilde{\mathbf{S}}_{\delta=\delta_{\text{Lim}}}$  is derived from the index  $\delta_{\text{Lim}}$  for which the estimator  $e_N$  is minimized (i.e., for which the signal-to-noise ratio reaches its highest value). From Figure 2, it is derived that  $e_N$  is minimized when  $\delta_{\text{Lim}} = 12$  for the static animal. When the animal is moving in the arena, the highest signal-to-noise ratio is reached when  $\delta_{\text{Lim}} = 9$ . Once the clutter is removed, the range of the sheep from the radar may then be derived at each time  $t_k$  from detecting the highest magnitude in beat frequency spectrum stored in the  $k$ th row of the matrix  $\tilde{\mathbf{S}}$ .

## 5. RADAR TRACKING OF A SHEEP IN THE PRESENCE OF THE FARMER

When a farmer is behind the arena wall, the resulting non-stationary clutter may obscure the radar signature of the sheep and render the animal detection and ranging very difficult. For illustration purpose, Figures 4(a) and (b) show the picture and radar image obtained when the sheep and the farmer move within the scene. At time  $t_{370} = 37$  seconds, both sheep and farmer generate high echoes in the image of matrix  $\tilde{\mathbf{S}}_{\delta}$ . At this particular moment, the echo from the farmer (at range of 9 meters) is stronger than the echo of the sheep (at range of 4 meters) and consequently, the highest magnitude of the beat frequency spectrum stored in the 370th row of the matrix  $\tilde{\mathbf{S}}_{\delta}$  is not associated with the sheep range from the radar. As a result, the tracking of this peak generates false detections. To overcome this issue, additional signal processing is needed. First, in order to remove remaining spurious clutter from the image of matrix  $\tilde{\mathbf{S}}_{\delta}$ , a low-pass filtering may be applied at each time  $t_k$  (the cut-off time is set to 270 milliseconds). The resulting filtered matrix is shown in Figure 4(b). Two subsequent steps are then proposed for completing the above-mentioned 3 steps.

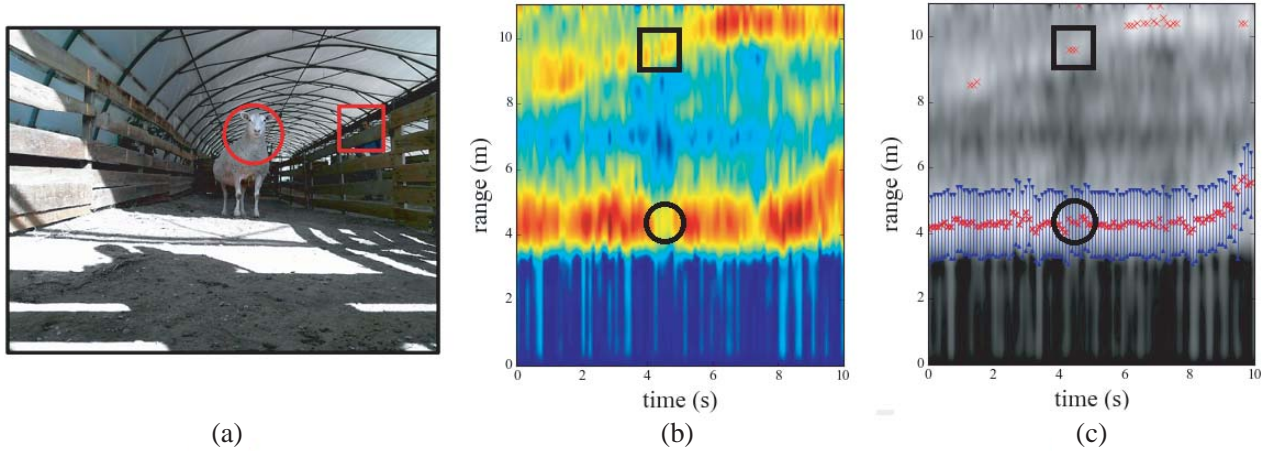


**Figure 4.** (a) Picture taken during the measurement. The sheep and the farmer are highlighted respectively by a circle and a square. (b) The resulting filtered image of the matrix  $\tilde{\mathbf{S}}_{\delta}$ , with the corresponding ranges of the sheep (circle) and the farmer (square). (c) Red crosses correspond to maximal values and the highest magnitude  $\hat{p}_k^{\text{max}}$  of the sheep is obtained inside the blue interval  $\Delta$ .

### 5.1. Step n°4: Nearest Neighbor Algorithm for Removing the Farmer Clutter

At each time  $t_k$  only the two highest magnitudes in beat frequency spectrum of the matrix  $\tilde{\mathbf{S}}_{\delta}$  are detected (see the red crosses in Figure 4(c)). From steps n°1 to n°3, the range of the sheep is estimated

at time  $t_1, t_2, \dots, t_K$ . In order to remove the unwanted magnitude associated with the backscattering from the farmer, a nearest neighbor algorithm is applied here. This algorithm consists of searching the highest magnitude  $\tilde{p}_k^{\max}$  at time  $t_k$  in the beat frequency spectrum in a time interval  $\Delta$  centered at the sheep range estimated at the previous time  $t_{k-1}$ . The interval  $\Delta$  (see blue segments in Figure 4(c)) is given by  $T_{\text{Meas}} \times v$ , where  $v$  and  $T_{\text{Meas}}$  denote respectively the maximal speed of the animal ( $v \cong 10$  m/s) and the measurement time (that is,  $T_{\text{Meas}} = 2T_M = 10$  milliseconds). Assuming that the farmer's echo is out of the time interval  $\Delta$ , such time gating technique allows removing the farmer clutter and measuring the sheep range at time  $t_k$  from the range estimated at previous time  $t_{k-1}$ . However, if the farmer's echo is included within the interval  $\Delta$ , false detections may occur and the estimated sheep range might be erroneous. The next step consists of removing such eventual detection ambiguities.

### 5.2. Step n°5: MULTiple Signals Classification Algorithm for Enhancing the Farmer Clutter Mitigation

In the case illustrated in Figures 5(a) and (b), the farmer clutter lies within the area occupied by the sheep and consequently, the actual sheep range (represented with a green line) may be inaccurately estimated. To overcome this specific issue, a simple solution consists of selecting not only the highest peak at time  $t_{48}$ , but also the two higher peaks denoted by  $\tilde{p}_k^{\max}$  and  $\tilde{p}_k^{\text{sec}} (< \tilde{p}_k^{\max})$ . The peak  $\tilde{p}_k^{\text{sec}}$  is selected only if its magnitude is not negligible compared with  $\tilde{p}_k^{\max}$ . Next, the Direction-of-Arrivals (DoAs) of the backscattered signals associated with these two peaks are derived from using the 2D MUSIC (MULTiple SIGNALS Classification) algorithm [26]. This algorithm allows deriving the azimuthal arrival angles of these two signals from the phase differences measured at the two reception radar channels. The accuracy of the DoA estimation increases as the number of channels increases, but only two channels are sufficient for deriving the two azimuthal angles  $|\Phi_1|$  and  $|\Phi_2|$  ( $|\Phi_1| < |\Phi_2|$ ) of signals backscattered by the sheep and the farmer. As the farmer and the sheep are respectively outside and inside the arena during the measurement, the smaller azimuthal angle  $|\Phi_1|$  unambiguously indicates the direction in which the sheep is present, while the larger azimuthal angle  $|\Phi_2|$  estimates the direction in which the farmer is present. Figure 5(c) displays the radar image after the DoA filtering of farmer clutter, represented by blue crosses. A Kalman filter [27] is applied on the detected highest echoes for removing remaining residual noise in the radar image. The resulting estimation of the sheep range is displayed as a function of time in Figure 5(c) with green dots. We observe a significant improvement of the measurement accuracy in the estimation of the sheep range at each time  $t_k$ .

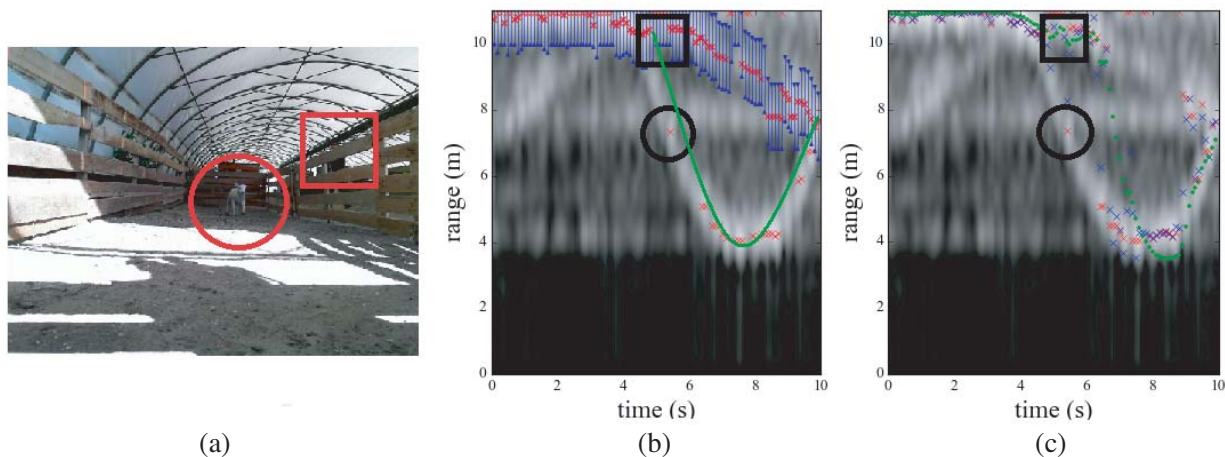


**Figure 5.** (a) Picture taken during the measurement. The sheep and the farmer are highlighted respectively by a circle and a square. (b) The resulting filtered image of the matrix  $\tilde{\mathbf{S}}_\delta$ , with the corresponding ranges of the sheep (circle) and the farmer (square). The green line represents the true range of the sheep and an error of tracking is made by focusing on the position of the farmer. (c) Red crosses correspond to maximal values and the blue crosses the position recorded after the DoA filtering. Green dots represent the position of the sheep after applying the Kalman filtering.

## 6. RADAR TRACKING OF ANIMALS WITH VARIOUS SIZES

The proposed radar technique may detect moving animals with various sizes (e.g., lamb of 50 centimeters long; ewe of more than 1m long) without performances degradation. Monitoring the range of the youngest animals in the enclosed arena is possible and may allow predicting the adult behavior. Such information could be used in breeding systems for selecting animals with high levels of sociability early during development and improving maternal behavior in adults. For illustration purpose, a lamb and a ewe were placed in the arena. We applied steps n°1 to n°5 the estimated ranges from the radar of these moving animals as a function of time. At the bottom of Figure 6(a) it can be clearly observed that the ewe keeps constant positions during at least 10 seconds while the lamb behavior (see the top of Figure 6(b)) is characterized by round trips along the arena. Such simultaneous range measures of ewes and lambs in standardized behavioral tests will provide reliable information to quantify social interactions. Such interaction between ewes and lambs is crucial just after lambing for the development of an adapted maternal behavior to ensure good suckling and lamb survival. In livestock, breeders are interested in improving maternal behavior in order to reduce labor and mortality of neonates which remains a major limitation for economic sustainability of several farms.

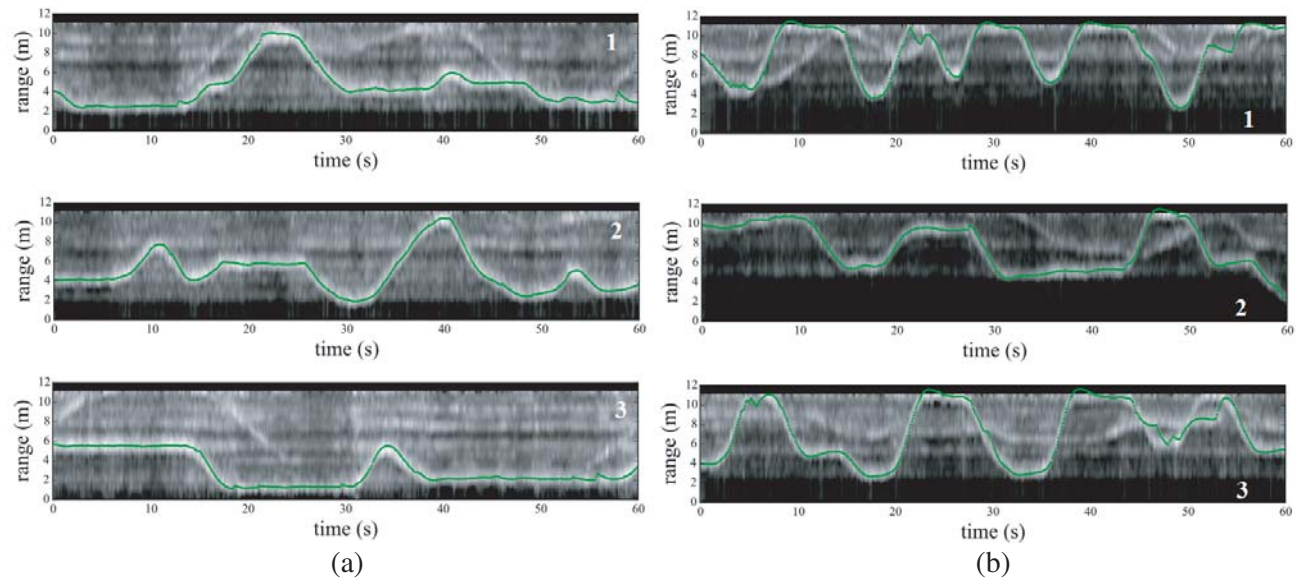


**Figure 6.** Estimated range from the radar (green lines) of (a) a ewe (a) and (b) a lamb inside the arena. These measurements are recorded separately during 1 minute with a time step of 100 milliseconds.

## 7. CONCLUSION

We report a new approach to estimate the range of moving animals from an FM-CW microwave radar using a methodology for removing the undesirable electromagnetic clutter from the radar image in the context of animal production research. The range variation of a single ewe, or even a smaller lamb, is estimated without using electronic tags (e.g., radio frequency identification tags). We use the SVD technique to remove clutters from the electromagnetic signal backscattered by the scene and to derive the successive ranges of animals up to 12 meters. These ranges are recorded and can be advantageously used to quantify animal behavior with high accuracy. Other external moving electromagnetic scatterers (such as farmers moving outside the arena) that may degrade the measurement accuracy were removed using the DoA analysis and MUSIC algorithm. While we introduced and experimentally validated here the application of FM-CW radars for automated analyses of sheep ranging in a standardized behavioral test for genetic studies and selection, our approach can readily be expanded to a wider range of animals and experimental contexts, thereby holding considerable promises for a broader use of



radars for quantifying animal movement in behavior research. For instance, tracking of smaller animals than a lamb is technically sound using FM-CW radars operating at higher frequencies that are already commercially available. Future development of our radar application could also combine multiple FM-CW radars to record animal trajectories in several dimensions simultaneously, thereby opening the possibility to track the spatial movements of multiple walking animals in 2D or flying animals in 3D with unprecedented high accuracy in the lab and in the field, an approach that is not possible with current automated behavior tracking methods.

## ACKNOWLEDGMENT

The authors acknowledge all the staff of the INRA experimental farm Langlade (Pompertuzat, France) for their involvement in the experiments.

## REFERENCES

1. Branson, K., A. A. Robie, J. Bender, P. Perona, and M. H. Dickinson, "High-throughput ethomics in large groups of *Drosophila*," *Nature Methods*, Vol. 6, 451, May 2009.
2. Weissbrod, A., A. Shapiro, G. Vasserman, L. Edry, M. Dayan, A. Yitzhaky, L. Hertzberg, O. Feinerman, and T. Kimchi, "Automated long-term tracking and social behavioural phenotyping of animal colonies within a semi-natural environment," *Nature Communications*, Vol. 4, Jun. 2013.
3. Woodgate, J. L., J. C. Makinson, K. S. Lim, A. M. Reynolds, and L. Chittka, "Life-long radar tracking of bumblebees," *PLOS ONE*, Vol. 11, No. 8, 1–22, 2016.
4. Strandburg-Peshkin, A., D. R. Farine, I. D. Couzin, and M. C. Crofoot, "Shared decision-making drives collective movement in wild baboons," *Science*, Vol. 348, No. 6241, 1358–1361, 2015.
5. Henry, M., M. Bguin, F. Requier, O. Rollin, J.-F. Odoux, P. Aupinel, J. Aptel, S. Tchamitchian, and A. Decourtye, "A common pesticide decreases foraging success and survival in honey bees," *Science*, Vol. 336, No. 6079, 348–350, 2012.
6. Balci, F., S. Oakeshott, J. L. Shamy, B. F. El-Khodori, I. Filippov, R. Mushlin, R. Port, D. Connor, A. Paintdakhi, L. Menalled, S. Ramboz, D. Howland, S. Kwak, and D. Brunner, "High-throughput automated phenotyping of two genetic mouse models of Huntington's disease," *PLOS*, 2013.
7. Rushen, J. and A. M. de Passille, "Automated monitoring of behavioural-based animal welfare indicators," *Animal Welfare*, Vol. 21, 339–350, 2012.
8. Pinkiewicz, T. H., G. J. Purser, and R. N. Williams, "A computer vision system to analyse the swimming behaviour of farmed fish in commercial aquaculture facilities: A case study using cage-held Atlantic salmon," *Aquacultural Engineering*, Vol. 45, 20–27, Jul. 2011.
9. Boissy, A., S. Ligout, D. Foulquie, A. Gautier, C. Moreno, E. Delval, D. Francois, J. Bouix, A. Boissy, S. Ligout, D. Foulquie, A. Gautier, C. Moreno, E. Delval, D. Francois, and J. Bouix, "Genetics of behavioural reactivity in sheep: A strategy for combining animal welfare and efficiency of production," *14emes Rencontres Autour des Recherches sur les Ruminants*, 301–304, Paris, Dec. 2007.
10. Hazard, D., J. Bouix, M. Chassier, E. Delval, D. Foulqui, T. Fassier, Y. Bourdillon, D. Francois, and A. Boissy, "Genotype by environment interactions for behavioral reactivity in sheep," *J. Anim. Sci.*, Vol. 94, 1459–1471, Apr. 2016.
11. Boissy, A., J. Bouix, P. Orgeur, P. Poindron, B. Bib, and P. Le Neindre, "Genetic analysis of emotional reactivity in sheep: Effects of the genotypes of the lambs and of their dams," *Genet. Sel. Evol.*, Vol. 37, 381–401, Aug. 2005.
12. Noda, T., Y. Kawabata, N. Arai, H. Mitamura, and S. Watanabe, "Animal-mounted gyroscope/accelerometer/magnetometer: In situ measurement of the movement performance of fast-start behaviour in fish," *Journal of Experimental Marine Biology and Ecology*, Vol. 451, 55–68, Feb. 2014.

13. Dell, A. I., J. A. Bender, K. Branson, I. D. Couzin, G. G. de Polavieja, L. P. J. J. Noldus, A. Prez-Escudero, P. Perona, A. D. Straw, M. Wikelski, and U. Brose, "Automated image-based tracking and its application in ecology," *Trends in Ecology & Evolution*, Vol. 29, 417–428, Jul. 2014.
14. Riley, J. R., A. D. Smith, D. R. Reynolds, A. S. Edwards, J. L. Osborne, I. H. Williams, N. L. Carreck, and G. M. Poppy, "Tracking bees with harmonic radar," *Nature*, Vol. 379, 29–30, Jan. 1996.
15. Lihoreau, M., N. E. Raine, A. M. Reynolds, R. J. Stelzer, K. S. Lim, A. D. Smith, J. L. Osborne, and L. Chittka, "Radar tracking and motion-sensitive cameras on flowers reveal the development of pollinator multi-destination routes over large spatial scales," *PLOS Biology*, Vol. 10, No. 9, 1–13, 2012.
16. Milanese, D., M. Sacconi, R. Maggiora, D. Laurino, and M. Porporato, "Design of an harmonic radar for the tracking of the Asian yellow-legged hornet," *Ecology and Evolution*, Vol. 6, No. 7, 2170–2178, 2016.
17. Ovaskainen, O., A. D. Smith, J. L. Osborne, D. R. Reynolds, N. L. Carreck, A. P. Martin, K. Niitepld, and I. Hanski, "Tracking butterfly movements with harmonic radar reveals an effect of population age on movement distance," *PNAS*, Vol. 105, 19090–19095, Sep. 2008.
18. Lvei, G., I. A. Stringer, C. D. Devine, and M. Cartellieri, "Harmonic radar — A method using inexpensive tags to study invertebrate movement on land," *New Zealand Journal of Ecology*, Vol. 21, No. 2, 187–193, 1997.
19. Pellet, J., L. Rechsteiner, A. K. Skrivervik, J. F. Zrcher, and N. Perrin, "Use of the harmonic direction finder to study the terrestrial habitats of the European tree frog (*Hyla arborea*)," *Amphibia-Reptilia*, Vol. 27, Mar. 2006.
20. Ligout, S., D. Foulqui, F. Sbe, J. Bouix, and A. Boissy, "Assessment of sociability in farm animals: The use of arena test in lambs," *Applied Animal Behaviour Science*, Vol. 135, 57–62, Nov. 2011.
21. Palandoken, M., "Compact bioimplantable MICS and ISM band antenna design for wireless biotelemetry applications," *Radioengineering*, Vol. 26, 917–923, Dec. 2017.
22. Atayants, B. A., V. M. Davydochkin, V. V. Ezerskiy, V. S. Parshin, and S. M. Smolskiy, *Precision FMCW Short-range Radar For Industrial Applications*, Artech House, 2014.
23. Piper, S. O., "Receiver frequency resolution for range resolution in homodyne FMCW radar," *Conference Proceedings National Telesystems Conference 1993*, 169–173, Jun. 1993.
24. Golub, G. and W. Kahan, "Calculating the singular values and pseudo-inverse of a matrix," *Journal of the Society for Industrial and Applied Mathematics Series B Numerical Analysis*, Vol. 2, 205–224, Jan. 1965.
25. Tivive, F. H. C., A. Bouzerdoum, and M. G. Amin, "A subspace projection approach for wall clutter mitigation in through-the-wall radar imaging," *IEEE Transactions on Geoscience and Remote Sensing*, Vol. 53, 2108–2122, Apr. 2015.
26. Belfiori, F., W. V. Rossum, and P. Hoogeboom, "Application of 2d MUSIC algorithm to range-azimuth FMCW radar data," *2012 9th European Radar Conference*, 242–245, Oct. 2012.
27. Kalman, R., "A new approach to linear filtering and prediction problems," *Transactions of the ASME — Journal of basic Engineering*, Vol. 82, 35–45, Jan. 1960.